Circularly polarized light emitting diodes

Michele Merelli[†*]

[†]*Zernike Institute for Advanced Materials, Rijksuniversiteit Groningen, The Netherlands*

E-mail: m.merelli@student.rug.nl

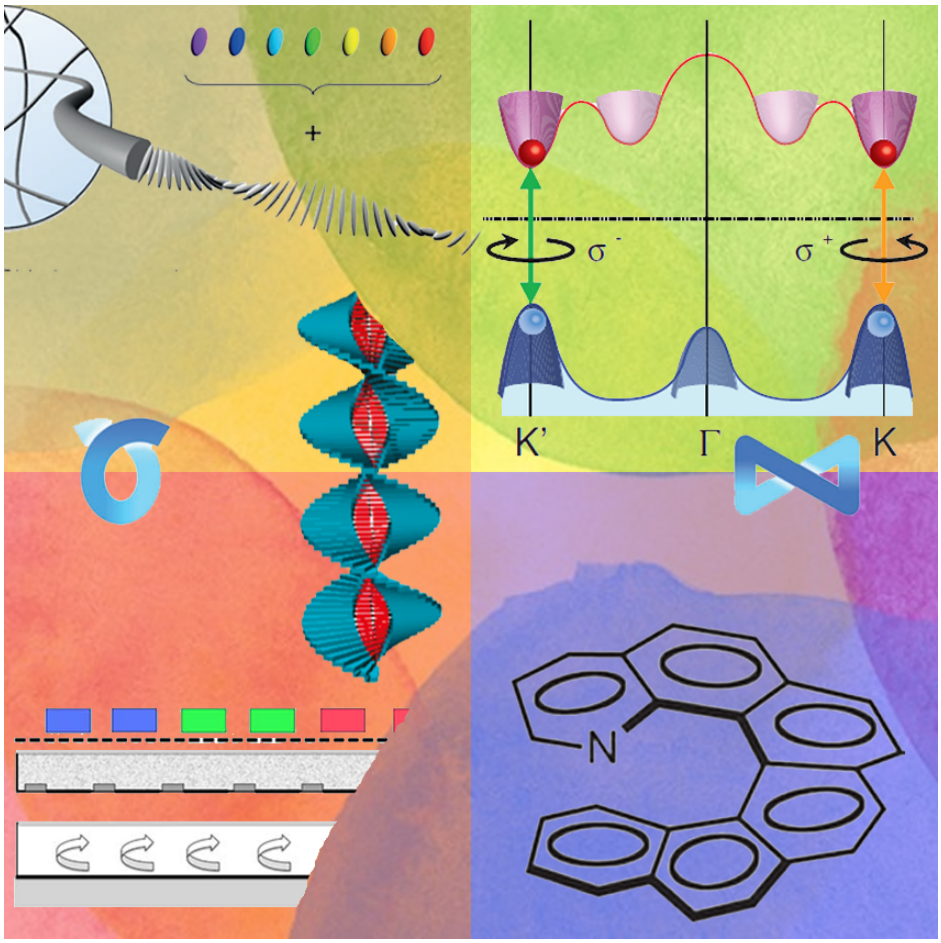

Research Paper - Top Master in Nanoscience

Supervisor: Thomas la Cour Jansen

Academic Year: 2016-2017

Abstract

The development of circularly polarized light emitting diodes (CP-LEDs) could expand the properties and the efficiency of LEDs, allowing their favourable application in fields like liquid crystals displays, biomedical imaging and spintronics. Most of the here reported studies will discuss about a subclass of organic LEDs (OLEDs). OLEDs are commercially interesting due to their light weight and solution processability. However, these are only few of the many improvements that OLEDs could supplement to the field. For instance, the organic active layer allows the system to integrate chirality, one of the most central molecular and *super*molecular property. We will mostly focus on several approaches that tried to use chirality of molecules, aggregates or templates to alter the emission process, resulting in circularly polarized luminescence (CPL). Also, we will report the developments of spintronics and low dimensional materials, that paved the way for a new type of CPL mechanism. Due to this mechanism, CPL is not directly correlated with the molecular morphology, but with conservation of momentum and quantum-mechanical selection rules. After an analysis comprising secondary parameters such as efficiency, integrability in existing technologies and costs, we will show that for systems based on helicenes and transition metal complexes the commercial scale-up requirements are already met.

Contents

Introduction

Light emitting diodes (LEDs) have been spreading for the last decades in multiple applications and fields, pulling an important revolution in terms of cost of energy, quality of lighting and environmental compatibility. Still, many applications of these devices are nowadays only dreamed of, and cannot be achieved with conventional LEDs. Fields like screen lighting,[1] 3D and stereoscopic visual systems,[1] spintronics,[2] medical and pharmaceutical care,[3,4] could benefit significantly from developments in this field. All of these requests have a common denominator: circularly polarized light (CP-light). The special properties of this particular type of polarization will be explained further in this paper, and also different polarizing mechanisms and types of interaction between light and matter will be explained. It is fair to say that some of the pulling objectives of this work, *i.e.* the possible applications, can be achieved even using linearly polarized light (LPL). However, for existing liquid crystals displays (LCDs), CP-light would allow higher technical performances, resulting in more bright, compact and less energy consuming devices.[5] When used for biomedical purposes, such as in imaging of tissues that exhibit birefringence,[3] circularly polarized light has significant advantages over the linearly polarized one, because the scattering events from the biological turbid media are less probable.[4] In other applications, as in high-resolution molecular chirality spectroscopy[6] and spin-communication systems,[2] CP-light is strongly needed and cannot be substituted by other modes of polarization.

In order to develop circularly polarized luminescence (CPL) from regular LEDs, many research groups tried to include particular materials in the conventional LEDs device structure. Before examining in depth our treatise, we need to make a particular remark, that holds for the majority of the possible applications. Independently of the proposed polarizing strategy, two key parameters have to be simultaneously optimized. These are the quantum yield (QY) and the dissymmetry factor (g_{lum}, a parameter that is helpful to evaluate the chiroptical activity). One of the main difficulties in this field is that these two parameters are intrinsically related: most of the times, the optimization of one property strongly and negatively influences the other one. For the principal purpose of this paper, that is improvement in LCDs back lighting, a luminance of at least 200 cd/m^2 and a g_{lum} not smaller than 0.1 could be set as good goals for a new generation of efficient displays. Together with these parameters, it will be important to bear in mind other general or application-specific goals. While for every type of application CPL over the entire visible range is an important requirement; thresholds about efficiency, weight, cost or complexity of device preparation could depend on the particular application.

Most of the here reported methods are based on solution processable techniques. In this category, the approaches are divisible in two main families: the chiral molecules or aggregates and the chiral template. In the first one, the emitting molecule or polymer is endowed of a chiral surrounding, aggregates in a spiral-like fashion or is blended with chiral species, showing optical activity. In the second one, the chirality is provided by a template, that accommodates achiral emitting chromophores. In conclusion of this paper, we will move

away from these systems to study the feature of solid state inorganic devices, for which CPL arise from different mechanisms.

In this paper, we will deal with supramolecular chemistry, quantum mechanics, electronic and photonic band theory for low dimensional materials and spintronic; subjects that find a common ground in nanoscience. It will be scientifically fascinating to understand the unexpected connections between different approaches and distant scientific fields.

Outline

- In **Section 1** after introducing light emitting diodes (**1.1**), we analyse CP-light and give a brief theoretical treatment of the origin of chiroptical activity to a molecular level (**1.2**). After this, LCDs screen technologies and their working principles are discussed as a pivotal example of possible application of CP-LEDs (**1.3**). In particular, we will show the main improvements that could be achieved with CP-LEDs. In addition, other peculiar examples of possible application, in field like spintronics or medical care, are given (**1.4**).

- In **Section 2** are presented CP-LEDs based on chiral organic molecules and aggregates with emphasis on the logical and historical developments that have led to new implementations. In particular, we will deeply focus on chiral side chains in conjugated molecules (**2.1**), cholesteric liquid-crystals (**2.2**) and chiral dopants such as small organic molecules (**2.3.1**) and metal-complexes (**2.3.2**). In conclusion, some recent approaches will be discussed (**2.4**).

- In **Section 3** are introduced some alternative, solid-state devices. In particular, we will talk about spin-LEDs (**3.1**), devices that show CPL when the spin density of state is modulated, and low dimensional transition metal dichalcogenides (TDMs)-based systems (**3.2**), exploiting valleytronic properties. A remark on the main differences between organic and inorganic devices will also be provided, with a discussion about some unique applications of these systems only.

1 Circularly polarized light: theory and applications

1.1 Light emitting diodes

Light emitting diodes (LEDs) are optoelectronic devices that, upon application of a forward electrical bias, favour the radiative recombination of electrons and holes resulting in emission of light (electroluminescence) (Fig. 1). LEDs based on inorganic (*p*-*n* direct band gap semiconductors junction) and organic (exploiting the potentiality of conjugated systems,[9] acting as active layer) materials are well-established devices. In recent year, they become extremely important for every-day application in, *e.g.*, devices screens' technology (active-matrix organic light-emitting diode (AMOLED) matrices, LCDs back lights) or environmental and task lighting, thanks to their low power consumption and long working lifetime.

1.2 Circularly polarized light: from molecules and aggregates

Conventional LEDs are unpolarized light sources. That is, the direction of the electric field (E) in the plane perpendicular to the the Poynting vector (direction of propagation) is not unequivocally defined. However, in optics there are particular sources or setups that can generate light with a controlled polarization. In this work, we will particularly focus on circularly polarized light (CP-light). CP-light is type of polarization of the electromagnetic wave for which the following relation describe the variation of the electric field (Fig. 2):

$$E(x,t) = E_0\,\mathrm{Re}[\hat{\boldsymbol{x}}e^{i(kx-\omega t)} + \hat{\boldsymbol{y}}e^{i(kx-\omega t+\pi/2)}] \tag{1}$$

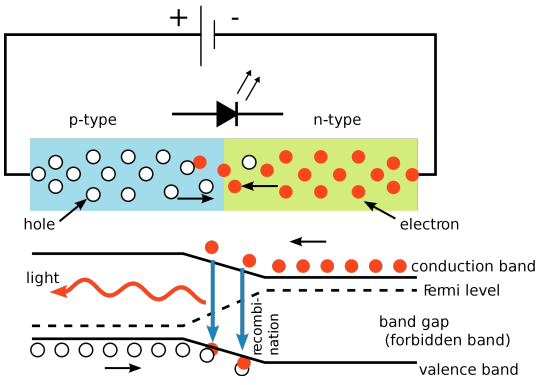

Figure 1: Band structure of a *p*-*n* junction diode, showing the working principle of the device. Holes and electrons recombine in the depletion region at the *p*-*n* interface, resulting in photon emission.[7]

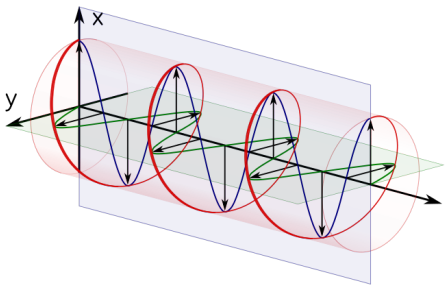

Figure 2: Scheme of right-handed circularly polarized light, showing the projections of the $\boldsymbol{x}$ (blue) and $\boldsymbol{y}$ (green) components of the electric field (projection method).[8]

in particular the $\boldsymbol{x}$ and $\boldsymbol{y}$ components of E are $\pi/2$ phase-shifted. That is, for circularly polarized light the ratio $\chi = \boldsymbol{E_x}/\boldsymbol{E_y} = \pm i$

In order to characterize and compare different devices efficiencies, two of the most important parameters are the circular dichroism (CD) and circularly polarized luminescence (CPL) and their respective dissymmetry factors (g_{abs}, g_{lum}). CD ($CD = \Delta\varepsilon$) tells about the differences in absorption of different handedness of CP-light, while CPL ($CPL = \Delta I$) studies the asymmetries in the emission:[10]

$$g_{abs} = \frac{\Delta\varepsilon}{\varepsilon} = \frac{\varepsilon_L - \varepsilon_R}{\varepsilon_L + \varepsilon_R} \qquad\qquad g_{lum} = \frac{\Delta I}{I} = 2\frac{I_L - I_R}{I_L + I_R} \tag{2}$$

with ε molar extinction coefficient and I intensity of the emitted light, for (R) right- or (L) left-handed polarization. The factor 2 added in g_{lum} is introduced for consistency, according to the definition of g_{abs}, that uses an average quantity of ε.

CD spectra are of fundamental importance when studying stereochemical compounds and assemblies. One of the most important features of CD data is the study of the sign variation in absorption close to the absorbing peaks, connected with the Cotton effect.[11] In particular, the analysis of type of Cotton effect, that is a change of sign of CD near the absorption peak, can help to discriminate different molecules or structures or different mechanisms for CD and CPL. Depending on the trend in the sign change, the Cotton effect is said to be positive (negative) if $\Delta\varepsilon$ near the absorption band is at first positive (negative) in decreasing the wavelength.

When analysing the molecular origin of CD, we need to consider the rotational strength, R, given by the Rosenfeld equation:[10,12]

$$R = Im[\,\langle\Psi_0|\hat{\boldsymbol{\mu}}|\Psi_n\rangle\ \langle\Psi_0|\hat{\boldsymbol{m}}|\Psi_n\rangle] \tag{3}$$

where $\hat{\boldsymbol{\mu}}$ and $\hat{\boldsymbol{m}}$ are the electric and magnetic transition dipole moment operators, while Ψ_0 and Ψ_n are the ground and n-excited states.

More specifically, the rotational strength is related experimentally to the CD and the dissymmetry factor by the relation:

$$R_{exp} = \frac{3hc10^3 ln(10)}{32\pi^3 N_A}\int\frac{\Delta\varepsilon}{\nu}d\nu \tag{4}$$

in which h is the Plank constant, N_A the Avogadro number, c the speed of light and ν is the frequency.

Taking into account the molecular theory, and defining θ the angle between the electronic and magnetic dipole moments, we can introduce another helpful expression of the dissymetry factor in absorption:[13]

$$g_{abs} = 4\frac{|\mathbf{m}||\boldsymbol{\mu}|}{\mathbf{m}^2 + \boldsymbol{\mu}^2}cos(\theta) \tag{5}$$

where $\boldsymbol{\mu}$ and $\mathbf{m}$ are the electronic and the magnetic transition dipole moments.

Riehl *et al.*[14] predicted a linear correlation between g_{abs} and g_{lum}. For this reason, especially if the vibrational relaxation can be excluded, the rotational strength and g_{abs} can be, to a good approximation, considered as the emission probability (also know as Kasha's rule). With these hypothesis, the dissymmetry factor g_{lum} can be defined as:

$$g_{lum} = \frac{R}{I^{(\alpha)}} \tag{6}$$

where I is the Fermi's golden rule in emission:

$$I^{(\alpha)} \propto \langle \Psi_0 | \hat{\boldsymbol{\mu}} | \Psi_n \rangle \, \Gamma(\omega - \omega^{(\alpha)}) \tag{7}$$

and $\Gamma(\omega - \omega^{(\alpha)})$ is a particular line shape function, centered at the frequency $\omega^{(\alpha)}$.

This background is especially important when considering small molecular dopants as active material like in **Section 2.3**.

Later, this theoretical frame was expanded in order to contemplate the contribution of CD and CPL of molecular aggregates. Various aggregate geometries and molecular building blocks have been studied and can be modeled with this treatment. Here, we focus on the π-stacked helical aggregates. In literature, this type of aggregates was first modeled using substituted chiral oligophenylenes (MOPV_n) as chiroptically active material (Fig. 3). When excitonic coupling is activated, the starting point is the Frenkel Hamiltonian:[15]

$$H = \sum_n \mathcal{E}_0 \, |n\rangle \langle n| + \sum_{m,n}{}' J_{mn} \{ |m\rangle \langle n| + |n\rangle \langle m| \} \tag{8}$$

in this expression, $\mathcal{E}_0$ is the energy of the ground state and the second term takes into account the coupling between the nth and the mth molecules, governed by the coupling parameter J_{mn} (a Coulombic interaction). The state $|n\rangle$ corresponds to the electronically excited chromophore n (S_2), all remaining cromophores are in their ground state (S_0). The prime on top of the summation requires that $m \neq n$.

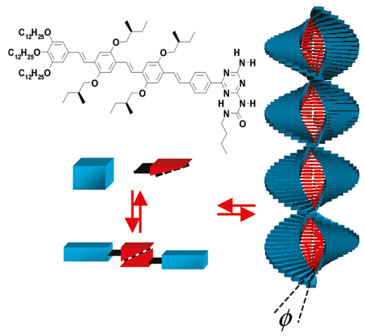

Figure 3: An illustrative representation of the chiral aggregate of MOPV_4.[16]

The eigenfunctions of this Hamiltonian can be expressed in the following way:

$$|\boldsymbol{k}\rangle = \sum_n \phi_{\boldsymbol{k}n} |n\rangle \tag{9}$$

where $\boldsymbol{k}$ is a quantum label assigned to the N one-exciton states; $\phi_{\boldsymbol{k}n}$ is the $\boldsymbol{k}$th wavefunction coefficient for the exciton state on molecule n obtained by diagonalizing the N×N matrix of the one-exciton Frenkel Hamiltonian. $|n\rangle$ is the basis state, where the molecule in n is excited, while all the other molecules are in their ground state.

The expression for CPL dissymmetry can then be generalized as follows:[17]

$$g_{lum}^{aggr} \equiv \frac{R^{aggr}}{I^{aggr,(\alpha)}} \tag{10}$$

with an extension to the aggregate state of the Fermi's golden rule[18]

$$I^{(\alpha)} = \frac{1}{\mu^2} |\sum_k \langle \boldsymbol{k}|\hat{\boldsymbol{M}}|G\rangle|^2 \Gamma(\omega - \omega^{(\alpha)}) \tag{11}$$

where $|G\rangle$ is the pure electronic ground state with all the chromophores unexcited, and the aggregate electric dipole moment, $\hat{\boldsymbol{M}}$, is a sum of molecular contributions:

$$\hat{\boldsymbol{M}} = \sum_n \hat{\boldsymbol{\mu}}_{\boldsymbol{n}} \qquad\qquad \hat{\boldsymbol{\mu}}_{\boldsymbol{n}} \equiv |n\rangle \langle G| \boldsymbol{\mu}_n \tag{12}$$

and each molecular electronic dipole moment, $\boldsymbol{\mu}_n = \mu[\cos(\phi n)\boldsymbol{i} + \sin(\phi n)\boldsymbol{j}]$ is considered directed mainly along the nth chromophore axis.

When the molecular magnetic dipole moment is neglected, the aggregate rotational line strength, R_{lum}^{aggr}, is expressed as

$$R_{lum}^{aggr} = \frac{k}{c\mu^2} \sum_{n,m} \boldsymbol{\mu}_n \times \boldsymbol{\mu}_m \cdot (\boldsymbol{r_n} - \boldsymbol{r_m}). \tag{13}$$

Here $(\boldsymbol{r_n} - \boldsymbol{r_m})$ is the distance between the nth and mth cromophore and k is defined as ω_{FC}/c, with ω_{FC} the Frank-Condon vertical transition frequency.

This is an expansion to the *super*molecular aggregates (*via* the Frenkel Hamiltonian) of the previously mentioned Rosenfeld equation, that was further extended with vibrational levels, disorder parameters and different coupling strengths and assembly lenghts.[17] However, the depicted theory is a good starting point for the analysis of chiral aggregates (**Section 2.1**).

1.3 Liquid crystal displays: a pivotal example

One of the fields that can benefit the most from improvements in CP-LEDs is liquid crystal screens (LCDs) technology. In these devices, the established device structure can be schematized as shown in Fig. 4a. The active layer, composed of a certain liquid crystal

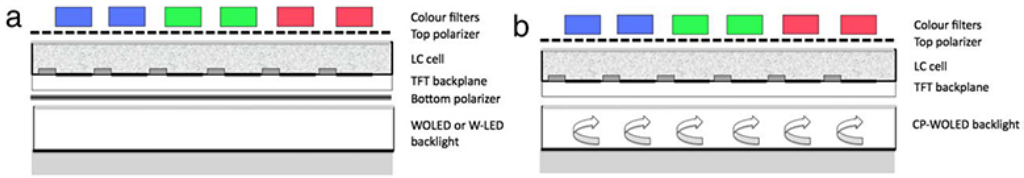

Figure 4: Comparison between a) existing LCDs technology and b) proposed working principle of new generation LCDs. In b) it is worth noticing the reduction in the number of polarizers, that can improve screen performances up to 50%.[1]

systems (with in-plane or twisted nematic switching layers), is sandwiched between two polarizers. By controlling the orientation of the mesophase of the active matrix, one can achieve a selection of colors and a control of the on-off state of single pixels.[19] In conventional LCDs, the main issue is the low efficiency caused by the two polarizers. In fact, starting from a non-polarized light source, half of the emitted light is loss in the interaction with the first polarizer. By introducing CP-LEDs in the back-lighting matrix (Fig. 4b), one of the polarizer could be removed, achieving the same device behaviour without this loss. Furthermore, these particular LEDs could be exploited for 3D vision systems, when coupled with passive CP glasses.[1]

1.4 Other possible applications

Besides the aforementioned main technological optimization that CP-LEDs could bring in our daily life, other fields can be strongly affected by improvements of these devices. Another important application of CP-LEDs could be molecular recognition and drug analysis.[3] In this case, improved examination of drug concentration and biological aggregates can be carried on. Providing other examples, CP-LEDs can optimize stereoscopic vision systems[20] and have application in new fields such as spintronics[2] (see also **Section 3**).

In order to achieve the challenging requests of the multiple applications shown, several methods have been proposed to tackle the problem. At first we will focus our attention on devices that take advantage of the chirality of various organic molecules or ensembles, in order to obtain CP-light emission. Later, we will explore other architectures, based on inorganic and solid state systems that exhibit CP-light emission. Since the mechanism of CP-light generation is connected with spin injection, these devices could be used not only for new generation LCDs, but also for spintronics applications.

2 Organic circularly polarized light sources

2.1 Chiral side groups in conjugated polymers

One of the first attempts in the field of CP-LEDs was to attach a chiral pendant side chain to π conjugated polymers, such as poly(thiophene) (PT) and poly(*p*-phenylene-vinylene) (PPV).[21,22] The main idea was that these moieties could lead to the formation of small chiral aggregates, with enhanced g_{lum}. In early works, it was clear that one of the interaction responsible for chiroptical activity was the Coulomb interaction, due to interchain exciton coupling: an interaction between dipole moments on neighbouring chains.[23] In particular, it was found that the typical signal in CD spectra, in case of this interaction, was a symmetric bisignate Cotton effect for the $\pi - \pi^*$ transition. The first working device based on these systems was proposed by Peeters *et al.*[24] They characterized poly(2,5-bis[(S)-2-methylbutoxy]-phenylene]vinylene) (BMB-PPV) emission and absorption spectra, showing CD and CPL in 1,2-dichlorobenzene solution. However, one of the main problems was the low solubility due to aggregation (0.05 mg/mL in chloroform), that strongly influenced the preparation procedure of these systems. In order to maintain the solution-processability, a racemic [(±)-(3R,3S)-(3,7-dimethyloctyl]oxy side group was introduced in the block copolymer. However, this substitution was found to considerably affect the dissymmetry factor of the emitted light. Moreover, several other issues arose when the device was fabricated *via* spin-coating. Since the formation of the film is strongly out of equilibrium, the chiroptical properties were further reduced, due to the decreased possibility of chain stacking compared to the slow cooling of active solution.

With further investigation, it became clear that the molecular arrangement of the chains in the active layer, as well as the precise shape of the assembly were crucial. However, for many years the precise mechanism of the origin of CPL was not certain and fully understood. The first rigorous investigation around this problem started with the work from Oda *et al.*[25] In this study, they analysed poly(fluorene) (PF)-based systems, in which the extent of the chirality in the pendant chain was varied. Comparing the CD spectra with previous works, in which the Cotton-effect lobes were symmetric (as predicted by *inter*chain exciton-coupling theory), discrepancies with this model were found (Fig. 5). At the same time, after sample annealing, higher g_{lum} values were observed. Even if these systems manifest also a liquid-crystalline (LC) transition, that we will discuss later (see **Section 2.2**), it was not clear why the chiroptical activity increased even for temperatures above the transition temperature (T_{LC}). In order to explain this behaviour, it was proposed that the backbone of the polymer, aided by thermal energy, could rearrange in a helical structure (induced chirality) (Fig. 6 c).[26]

This hypothesis was later confirmed by Hartree-Fock calculations,[29] in which high dissymmetry values were found even for *intra*molecular interactions in isolated polymer chains. Other studies reported the same mechanism (Fig. 6c).[28] Since the work of Oda *et al.*[25] proposed a method to reach high chiroptical effects namely g_{lum} as great as 0.25 in emission,

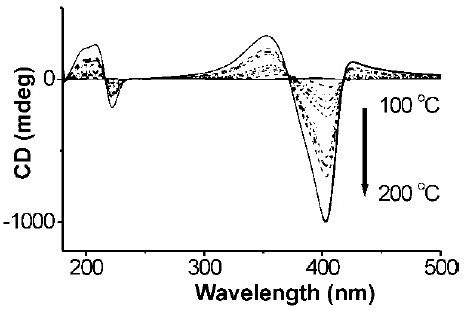

Figure 5: CD spectrum of a chiro-substituted PF that shows asymmetrical degree of circular polarization. This observation cannot be explained with regular excitonic coupling due to *inter*chain interactions.[25]

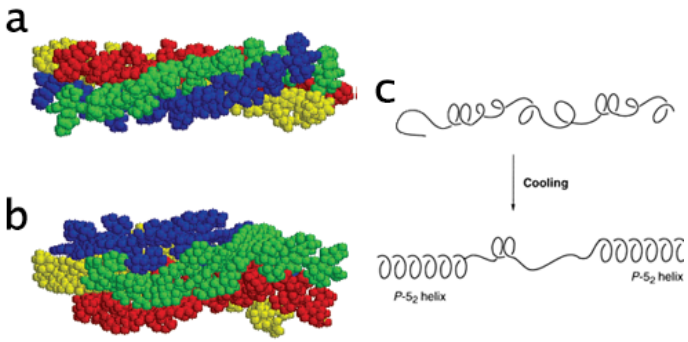

Figure 6: a), b) Molecular dynamic calculations for four fluorene nonamers. In a) the molecules arrange in an chiral and brained assembly, while in b) the aggregate of molecules, bearing a bulky pendant group, is not brained.[27] In c) is shown another type of possible arrangement, that leads *intra*molecular interactions as major coupling contributions.[28]

showing a 200-fold optimization of the system, a great interest was aroused. Therefore, even further investigation were carried on to deep the understanding of the proposed system. For instance, Geng. *et al.*[27] examined a subclass of these compounds (oligofluorenes) in order to facilitate the chiral-induced aggregation. At first, molecular dynamic simulations showed different packing structures depending on the chiral sidechains (Fig. 6 a, b). In particular, it was said that brained stacking should disfavour the cholesteric transition (a cooperative mechanism responsible for the chiroptical activity, as discussed in **Section 2.2**). Later analysis, however, demonstrated that the main mechanism for high dissymmetry factor was the cholesteric stacking (LC transition). Moreover, the helical arrangement was demonstrated not to be of fundamental importance in order to induce the LC transition: this transition was discovered even for linear compound like poly(*p*-phenyleneethynylene) (PPP).[30,31] This study chronology clearly shows the impervious development of a stable and systematic theoretical framework able to contemplate every aspect of these systems.

Before analysing the liquid-crystals approach, it is important to discuss another issue related with this method. π-mediated stacked designs are limited by the aggregation-caused quenching (ACQ), that reduces the quantum efficiency (QY) of these systems because of the population of non-radiative pathways.[32] Recent developments focused on another class of π-conjugated materials that show an opposite trend. For instance, silole and tetraphenylethene derivatives are characterized by the phenomenon "aggregation induced emission" (AIE). In one of the most important works of CPL in AIE molecules, Liu *et al.*[33] studied 1,1-dimethyl-2,5-bis[4-(azidomethyl)phenyl]-3,4-diphenylsilole emitting properties with different device schemes (casting, natural evaporation and incorporation in microfluidic channels).

Analysis of the CD spectra, as well as structural simulations demonstrated that in these systems exciton coupling mediated by π-π-stacking is not present. Furthermore, a combination of multiple hydrogen bonding and stereo-complementarity results in the maturation of helical nanoribbons. With these improvements, the group was able to accomplish high dissymetry factors ($|g_{lum}| = 0.32$) as well as QY as high as 81.3%.

Even if the astonishing improvements, provided for instance by AIE materials, several issues such as the aforementioned lack of theoretical explanation for complexly behaving systems, and the not straightforward relationship between chemical structure, supramolecular aggregation and optical activity has strongly obstructed the development of this device concept. In addition, the aggregation mechanism can also affect the solubility of these devices, compromising their solution-processability.

2.2 Liquid crystals and template-based

The pioneering findings of Oda *et al.* suggested another alternative and effective approach, consisting of systems based on LCs that could reveal high dissymmetric factors. In particular, chiral-nematic liquid crystals (N*-LCs, also known as cholesteric liquid crystals) were found to be more suitable in order to achieve the desired objectives of CD and CPL. The twisted nematic phase is a type of LC in which a helical arrangement of the chiral molecules or nanostructures is present. Specifically, a cholesteric phase can be described as a superposition of planes of nematic phase, each one twisted with the same angle. The pitch of the cholesteric (P_h) is defined as the length corresponding to half-helical rotation parallel to the the rotation axis, and plays an important role in the optical properties of the system. Another property of these systems is birefringence, related with different refractive indexes $\Delta n = (n_e - n_o)$ for extraordinary and ordinary directions.

One of the first theories of the intrinsic chiral activity of N*-LCs modeled the transmission of a cholesteric film in various frequency regions. In particular, it was found that, for the forbidden zone ($\varepsilon_{\perp}^{1/2} > (\omega/c|q|) > \varepsilon_{\parallel}^{1/2}$), only circularly and elliptically polarized light was transmitted by the film.[34] Here q is the magnitude of the reciprocal wave vector of cholesteric phase ($q = 2\pi\gamma/P_h$, with $\gamma = \pm 1$ corresponding to $\sigma_{\pm}$ left- or right-handed polarized light), and $\varepsilon_{\perp,\parallel}$ is the dielectric constant for light propagating perpendicular or parallel to the cholesteric axis. Later studies modeled fluorescence from the chiral nematic film itself, introducing a imaginary dielectric constant.[35] Following these theoretical studies, the first work in order to exploit these features was carried on by Chen *et al.*[36] In particular, they added small cromophores directly to the nematic matrix. The accepted explanation of the mechanism for the polarization of light in these system is that the nematic matrix mediates the helical arrangement of luminophores. In this way, light emitted from the luminophores is gradually and non-locally polarized, while travelling trough the nematic film, according to the detailed description provided by Good *et al.*[34] Due to the non-local mechanism for CPL, the degree of polarization in these systems is proportional to the thickness of the active layer. This helped to distinguish the various contributions due to different underlying mechanisms

for chiroactivity.

Two main issues are connected with out-of-resonance devices (λ_F not belonging to the forbidden zone). Primarily, the thickness of the active layer, being at least of 1-10 μm, severely limits the applicability and the integrability of this type of solution. Moreover, the aforementioned model cannot explain other features of the CPL spectra, that shows an inversion of the sign of g at the edge of the stop band.

In recent years, 1D photonic crystals band theory was shown to be another equivalent explanation and model of the cholesteric LC. Photonic crystals are regularly arranged nanostructures or molecules responsible for periodically modulated dielectric constants. The periodicity can affect photons similarly to the effect of ordered ions on electrons. This theoretical background is able to contemplate the in "resonance region" $\lambda_F/\lambda_{RF} = 1$, describing the forbidden zone as a bandgap. The dispersion relation in chiral LCs, treated as photonic crystals, is:[37,38]

$$\varepsilon_{av}(\omega_{\pm}/c)^2 = q^2[(\kappa^2+1) \pm \sqrt{4\kappa + 2 + K^2(\kappa^2-1)^2}]/(1-K^2) \tag{14}$$

where $\kappa = k/q_0$ and k are the relative and the absolute wave numbers associated with the radiation. The average dielectric function is defined as $\varepsilon_{av} = (\varepsilon_e + \varepsilon_o)/2$ and $K = (\varepsilon_e - \varepsilon_o)/(\varepsilon_e + \varepsilon_o)$. The photonic bandgap is found between $\omega_{max}(k=0)$ and $\omega_{min}(k=0)$, this yield $\lambda_{min} = n_o P_o$ and $\lambda_{max} = n_e P_o$ ($P_o = 2P_h$). The middle of the bandgap corresponds to $\lambda_{avg} = n_{av} P_o$.

According to this theory, CP-light that has the same chirality as the N*-LC phase is totally reflected. From Eq. 14, the range of reflection is limited to tens of nanometers, by the relation $\Delta\lambda = p\Delta n$. This could strongly discourage the application of single N*-LC in a white-emitting CP-LED, as required in LCDs back lights.

One of the milestone example of increased range of selective reflection was the work by Suzaki and coworkers.[39] In this study, a multilayered N*-LC device was able to transmit one-handed CPL, employing the "photon recycling" method. In practice, a unpolarized light source was used as emitting material and a metal, mirror-like material was placed at the back of the device. The forbidden electromagnetic waves were reflected by the N*-LC without change in handedness. The inversion of polarization occurred at the metal interface, so that the "recycled" CP-light could then be transmitted by the cholesteric film. In this concept, three separated layers with different dopants concentration provided different pitch geometries.

Even if the results of this device are promising, the three layers architecture is rather complex and introduces multiple new layers of liquid-crystal material. In addition, the device thickness, even if not reported, is expected to be considerable.

Later, other groups provided possible biomimetic solutions to the problem. Analysing the exoskeleton of the crab *Carcinus mænas*, it was discovered that the integrated cholesteric structure exhibits a pitch gradient.[40] Trying to mimic this behaviour, the group proposed the casting of two differently colored N*-LC, followed by annealing. This produced structures

with pitch gradient, able to reflect over a wide spectral range.

Several other approaches were carried on by Bobrovsky *et al.*, to change the properties of the pitch using photoswitchable molecules and controlling the UV exposure.[41]

Another interesting branch of research tried to join and condense the emitting and the N*-LC properties in one material. For instance, several synthetic approaches tried to modify conjugated polymer in order to achieve a N*-LC transition. In one crucial example,[42] the research group introduced chiral moieties in disubstituted poly(acetylene), yielding to the N*-LC transition. Elsewhere,[43] the transition to N*-LC phase was provided by the introduction of chiral dopants to the non-chiral LC phase (N-LC) (for instance the aforementioned PPP systems).

Inspired by these systems, another study expanded the potentiality of the "template-based" device structure: the molecular LC phase was substituted by a cellulose noncrystalline arrangement, doped with Eu nanoparticles as emitting moieties. In this way, a combination of property between this type of systems and the one presented in **Section 2.3.2**, was achieved.[44]

In conclusion, being the class with some of the highest dissymmetry factors, liquid crystal systems are promising example of CP-LEDs. However, the addition of a new liquid crystal component is disheartening, especially because the highest performances were obtained with the thickest device architectures. Moreover, secondary issues has to be taken into account, like the thermal stability of the LC phase and the thickness of the working device.

2.3 Doping with small molecules

2.3.1 Doping with chiral non-emitting compounds

Another possibility to obtain CP-LEDs, is to blend a conventional and achiral light emitting polymer with chiral small organic molecules (SOMs). One of the first examples, in this direction, was the blend proposed by Haraguki *et al.*[45] between a poly(thiophene) (PT) and a neutral polysaccharide (schizophyllan, SPG). For this system, a small g_{lum} was found (10^{-3}). One of the possible reasons could be the unfavourable conductivity properties of the polysaccharide chain, resulting in low device performances.[46] Upon the wide class of chiroactive (CP-SOMs), the most interesting class of materials as chiral doping molecule is the helicene family. These molecules have been characterized and studied for their optical activity,[13] as well as their effective enantiomeric separation. In particular, a molecular explanation of CD and CPL in helicenes was early found using time-dependent density functional theory (TD-DFT).[47] Using group theory (analysing A or B irreducible representations transitions), a symmetry-aided analysis of the typical electronic transitions and their properties was carried on. Transitions belonging to A group take place with μ_α and m_β in the direction of the z axis, while B-type transitions are relegated to the xy axis (Fig. 7).

The group was able to theoretically simulate CD and CPL spectra. As shown inFig. 7 and according to Eq. 4, the researchers derived a naïve, but consistent explanation for

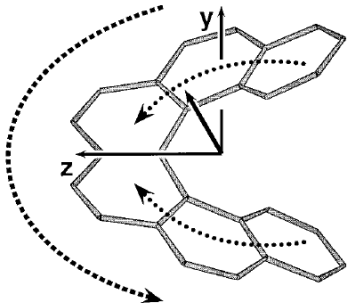

Figure 7: Naïve representation of the motion of electron clouds in A-type (dotted lines) and B-type (dashed lines) transitions.[47]

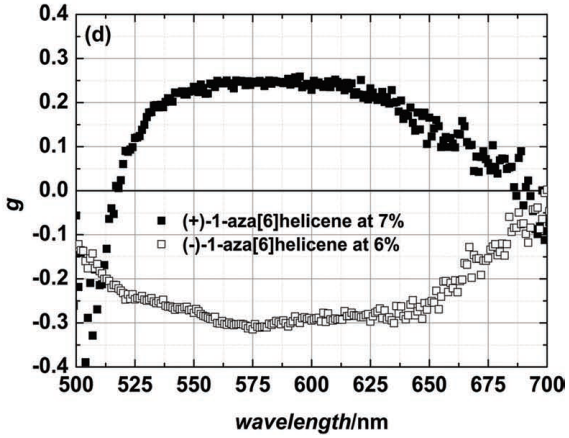

Figure 8: CPL spectrum of PFBT:(1-aza[6]-helicene) showing constant optical response over a wide spectral range. Notably, chirality of helicene molecule and sign of g_{lum} are directly correlated.[48]

positive g_{lum} values found for A-type transitions in left-handed helicenes. According to this explanation, this arises because μ and m are antiparallel, in the z direction. Later studies investigated, using DFT calculations, other helicene families ([4]helicenes and [7]helicenes) and the effect of substituents on their CPL activity.[49]

Recently, Yang and his coworkers proposed a blend of poly(fluorene-alt-benzothiadiazole) (PFBT) and 1-aza[6]-helicene, a particular helicene whom synthetic preparation can be scaled up efficiently.[48] With this system, a device showing a constant g_{lum} over a significant portion of the visible spectra was achieved (Fig. 8). Moreover, it was experimentally demonstrated a direct correlation between chirality of the helicene molecule and g_{lum} values. An analysis of the thickness dependency of the CP efficiency excluded other contributions, such as the transition to cholesteric-LC phase.

Recent investigations concentrated their attention on alternative helicene-like molecules. This derive from an important finding, that touches the heart of the discussed problem. Whenever a chromophore is twisted or bended, its emitting properties are strongly quenched. This process occurs with higher effectiveness in fully π-conjugated helicenes. For this reason, helicene-derivatives incorporating silole or fluorene moieties were shown to increase the QY.[50]

Working on the findings obtained from the helicene-like molecules, other chiral SOMs, such as chirally perturbed ketones, biaryl and chromophore-decorated C_2-symmetric cores were synthesised and incorporated in the achiral matrix.[13] (see also **Section 2.4**).

The blend of SOMs with emitting polymers is one of the most interesting approaches, as their production procedure can be integrated in conventional, solution processable preparation methods.

2.3.2 Ion complexes

Following the ideas and the concepts introduced in **Section 2.3.1**, different groups, instead of inserting a non-emissive chiral molecule, based their work on ion-complexes. Several ion complexes, belonging to different groups such as lantanides(III) (Eu(III)) and transition metals (Pt, Ir) were investigated. An important characteristic of this approach is the sharp CPL emission (in terms of wavelength) due to the characteristic transitions of the ion. Another feature is the potentially enhanced QY, obtained with phosphorescence (PH) luminescence: the previously mentioned organic systems (such as PF) cannot emit from the triplet-excited state. Thus, according to spin-statistic, are limited to 25% in internal quantum efficiency.[51] In compounds embedding heavy metals, this limitation is lifted due to spin-orbit coupling.

Talking about the subclass of lantanide(III) complexes, Muller *et al.* collected in a review the features of these compounds.[6] In particular, in these systems are found high dissymmetry factors (as high as 1.38) and sharp emission transition, resulting in circularly polarized and highly saturated color light emission. The origin of CPL arises from two different contribution. The main strategy to reach chiroptical activity is to place the Ln(III) ion in a chiral environment (as shown in Fig. 9), with ligand antenna showing at least one asymmetric carbon. Further increase in the CPL can be explained considering the $f - f$ transitions obeying magnetic-dipole selection rules, that give high g_{lum} according to Eq. 5.[52]

A clear example of the use of lantanide-based systems is a recent work by Zinna *et al.*[4] In this study, the focus was on Eu(III) complexes (namely $CsEu(hfbc)_4$) blended in a poly-

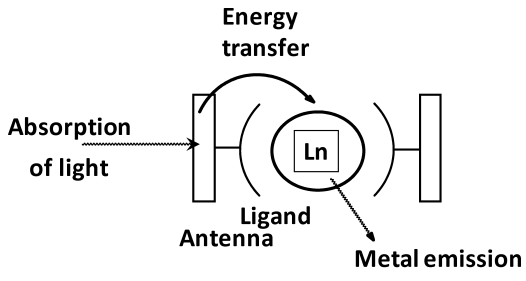

Figure 9: Scheme of the metal-ligand system, in which the ligand acts as an antenna, absorbing external radiation. This is re-emitted by the metal, after energy transfer.[6]

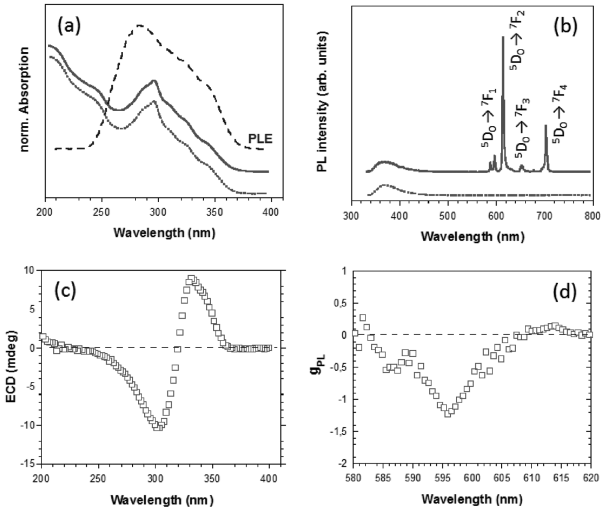

Figure 10: Absorption, ECD, PL and CPL spectra of the complex $CsEu(hfbc)_4$ in TCTA. High g_{lum} togheter with sharp electronic transitions are found, making this proof-of-concept device suitable for monochromatic CPL sources.[4]

mer matrix (tris(4-carbazoyl-9-ylphenyl)amine, TCTA). From the analysis of the spectral properties of the blend, the group found suggestions about the origin of the polarization of the light. In particular, comparing ECD (electronic circular dichroism) of the complex in solution and in the polymer matrix, they concluded that the chiroptical properties of the compound were maintained even in the device. Particular transition, such as $^5D_0 \rightarrow {}^7F_1$ at $\lambda = 595$ nm and $^5D_0 \rightarrow {}^7F_2$ at $\lambda = 611$ nm showed respectively -1.21 and +0.16 g_{lum} values (Fig. 10).

Further optimizations were carried out in order to increase the efficiency of the device. For all the architectures utilizing a metal anode, back-reflections of the emitted light causes an inversion of the polarization of the light, resulting in a decrease of g_{lum}. For this reason, an interfacial layer (IL) was inserted between the anode and the active material, in order to shift the recombination zone further away form the anode. Due to the matching in the band gaps, an optimization of the holes injection were accomplished. Since the metal-centered transitions have low QY, these systems need improvements in order to be able to find practical applications. However, with the IL optimization, the QY was increased by one order of magnitude in one year, with respect of proof-of-concept device.[53] The IL technological solution could be introduced to augment the efficiency of other CP-LEDs with a similar device structure.

Other systems based on Pt complexes (platinahelicenes)[54] recently demonstrated the applicability of chiral ion-complexes in large scale production, providing also an elegant connection between purely organic studies and metal complexes. In particular, the PH-OLED (phosphorescent organic LEDs) fabricated with chiral platinahelicene had a luminescence higher than 200 cd/m^2 (considered the threshold for displays), combining high g_{lum} and luminescence, even if the external quantum efficiency (EQY) could be potentially improved (from 10% to 30%).[55]

In conclusion, these systems are, for the case of transition metal complexes, promising example of a fruitful combination of high QY and g_{lum}, that can be easily integrated in nowadays technological solutions. However, the design of chiral ligand-complexes is not trivial and several problems can arise, such as pseudoracemization that suppress CPL activity.[56] Also, the CP-spectral range in emission is usually narrower, compared to other methods.

2.4 Recent investigations

After having shown many established methods and designs, it is now worth mentioning some recent experiments and directions. One of the other remarkable approaches is to transfer chirality from a chiral solvent to achiral molecules.[57,58] Another class of materials consists of small molecules able to emit from the triplet state, based on the effect of thermally activated delayed fluorescence (TADF). Recently a chiral perturbing unit was attached to them, yielding to a class of systems that can potentially achieve high QY as well as high dissymmetry factors.[59] In a different study, Goto *et al.* doped a chiral nanofibrillar template of L-glutamic acid derivatives with known cromophores. Selecting the proper dye led to wide

emission spectra.[60]

These recent methods enlarge the collection of possible ways for the design of high-performance devices, even if they are presented only as proof-of-concept design and they do need optimizations.

3 Alternative inorganic approaches

Simultaneously to the organic counterpart, interesting alternative approaches based on solid state devices were analysed during the years. In particular, these systems show possible applications and device characteristics that are not present in the previously described, organic counterpart. The general and pictorial explanation of the generation of CPL, in these systems, is connected with the conservation of angular momentum during the recombination process.[61] Since the total momentum of the electron-heavyhole pair is transferred to the generated photon, a total angular momentum $J = +1$ results in a σ_+ circularly polarized light (left circularly polarized). Conversely, for an electron-hole pair with $J = -1$, the emitted radiation is σ_- polarized (right-handed).

With this background information in mind, we can briefly explore the intriguing characteristics of solid state devices.

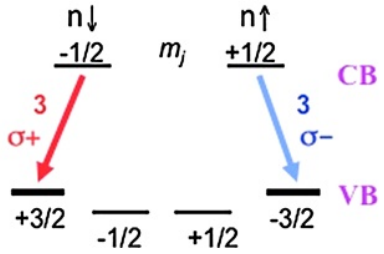

Figure 11: Diagram of the quantum-mechanical selection rules for vertical injection (Faraday Geometry) at the base of CPL generation in spin-LEDs.[61]

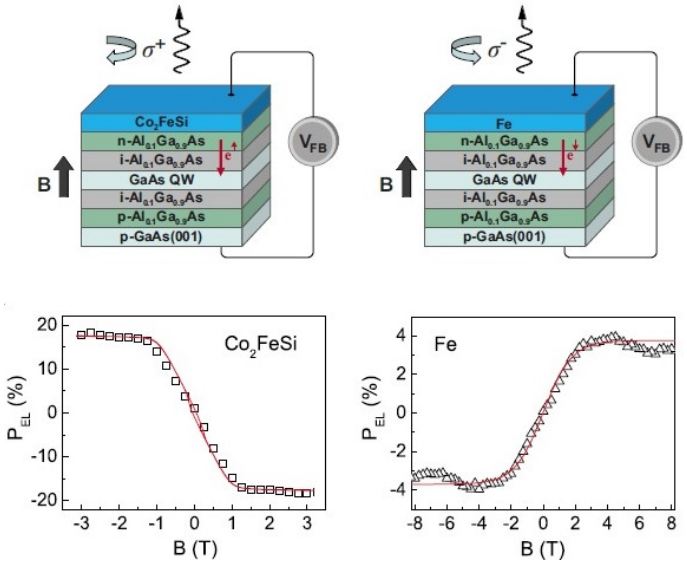

Figure 12: Schematic representation of a spin-LED system in Faraday geometry, showing CP light output (P_{EL}). It is worth noting that the light polarization can be controlled, changing the direction of the applied magnetic field.[2]

3.1 Spin-LEDs

Spin-LEDs are optoelectronic devices that emit CP-light. In general, whenever there is a dissymetry in the population of different spin states, the allowed recombination channels (considering non-degenerated levels in the valence band, for strained growth or quantum confinement)[62] generate CP-light (Fig. 11). For instance, a spin source can inject spin-polarized current in a *p-i-n* diode composed of one or multiple quantum wells (QWs) (Fig. 12). Since the selection rules for vertical spin injections are well established and known, the most used experimental configuration is the Faraday geometry, in which a magnetic field is applied perpendicularly to the QW. However, for many spin-sources thin film materials, a magnetization out-of-plane is hardly accomplished, especially without the application of high magnetic field (1-10 T).

The need of an high external magnetic field, together with the low working temperature of these systems strongly thwarted their applicability. However, in recent works CP-light was obtained even at room temperatures, using spin-injecting materials working in remanence (without the need of magnetic field) reaching 8% of light polarization.[63,64] Even if the degree of polarization for these systems is far below the organic counterpart, they are an unique example of transmission of information between spin-based devices.[2]

3.2 Solid state devices

Another class of promising materials is based on transition metal dichalcogenides (TMDs) like MoS_2 or WSe_2. From band theory, these systems (especially when quantum confined) present two equivalent interband transitions (K' and K in the hexagonal Brillouin zone) with different spin and momentum properties. In particular, the conduction band shows $l = 0$ corresponding to the *d*-states of Mo or W, thus the associated momentum is $m_{\pm} = \pm 1$ at $\mathbf{K}_{\pm}$. The valence band has quantum number equal to $m_{\pm} = 0$. For this reason, these

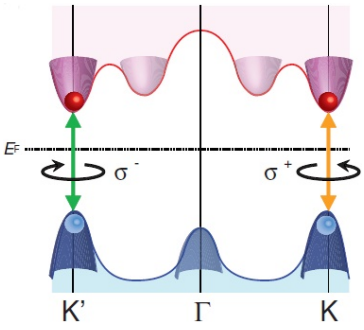

Figure 13: Sketch of valley-mediated selection rules that are responsible of CPL in TMDs materials.[65]

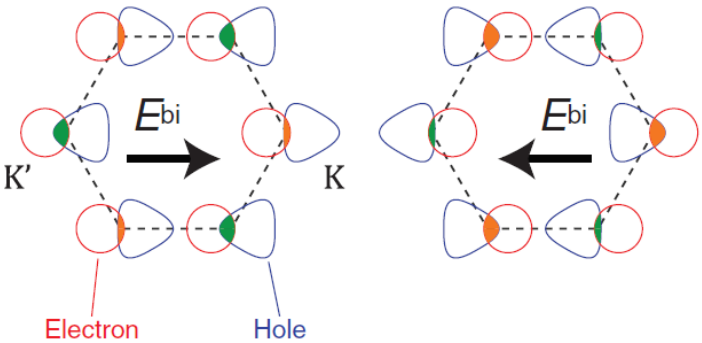

Figure 14: Illustration of the shift in hole and electron distribution, for different orientation of the electric field. Orange and green areas represent the overlap of K and K' valleys.[65]

systems show a valley-selective CPL (Fig. 13).[66,67]

Recently, Zhang *et al.* tried to exploit this peculiar behaviour, studying the possibility of electrically controlled CPL emission. First, they gated the device with ionic liquid as dielectric and cooled it down below 160 K (below the solid-liquid transition temperature), to guarantee the stability of the ambipolar behaviour. After this step, they successfully demonstrated that, applying differently-oriented source-drain bias on the ambipolar *p-i-n* yields to different CPL characteristics.[65] A semiclassical transport explanation of this phenomenon was provided: the applied field shifts the distribution of holes and electrons, varying the overlap and the efficiency of recombination since the carrier distributions are non-equivalent (Fig. 14). Similarly to spin-LEDs, these devices show low efficiencies, but the possibility to electronically control the output characteristics is unique.

Even if the device structure of these solid state approaches is considerably more complex and requires complex manufacturing instruments, these systems certainly show promising features, such as the electronic control of polarization, or application, such as spin-communication, deserving further investigation and attention.

Conclusions

After having discussed all the different approaches that have been investigated in the last two decades, it is worth summarizing the features and the characteristics of these systems. In doing so, we collected all the important parameters of the previously treated devices. As summarized in Table 1, the discussion about the results and the methods is multiparameter-dependent and can also be affected by the type of application. Since one of the main objectives of this work is to find suitable alternative and cost effective liquid crystals display (LCD) backlights, at first we will summarize on the results with this prospective.The requirements for this application are a wide spectral range $\Delta\lambda$ and high luminance or quantum yield (QY). This combination of necessities strongly affects the applicability of many of the described methods, that are limited at least for one of the required parameters. While in back lighting there is no threshold condition for the dissymmetry factor in emission g_{lum}, as per cent efficiency improvements can be reached even with small values (0.1), the same does not hold for luminance and spectral range. In order to have an efficient white back light, the selected system must display circularly polarized luminescence (CPL) over the full visible range ($\Delta\lambda$ = 390-700 nm). Moreover, as previously mentioned the luminance has to be greater than 200 cd/m^2. For this reason, only molecules showing "aggregation induced emission" (AIE), liquid crystals and helicene or Pt-complexes can be applied. These parameters are a necessary, but not sufficient condition for the applicability of the methods. In

Table 1: A summary of all the important parameters of a selection of some of the most promising designs analyzed in this paper. The acronyms correspond to different methods or approaches: conjugated polymers with chiral pendant group (PCP), aggregation induced emission systems (AIE), cholesteric liquid crystals (N*-LC), doping of achiral matrix with chiral molecules (CM) and complexes (CC). Inorganic approaches are also reported (IA).

Material	*Method*	g_{lum}	QY [%]	luminance [cd/m^2]	λ [nm]	Ref.
Poly(p-phenylene vinylene)	PCP	1.3 $\cdot 10^{-3}$	-	-	-	[24]
Silole with sugar pendants	AIE	0.32	81.3	-	420-620	[33]
Poly(fluorene)	N*-LC	0.25	-	-	-	[25]
Poly(p-phenylene)	N*-LC	0.23	-	-	380-520	[43]
Three-layered reflector	N*-LC	1.6	-	1500	450-650	[39]
Poly(acetylene)	N*-LC	0.23	30	-	450-530	[68]
YVO_4:Eu^{3+} and cellulose	N*-LC	0.3	2.6	-	620-630	[44]
Helicenes-like molecules	CM	0.3-0.5	-	3000	-	[48]
Pt-complex	CC	0.38	10	370	570-700	[54]
Eu-complex	CC	1.0	0.05	-	580-600	[4]
Spin-LED	IA	0.03	-	-	-	[63,69]
WSe_2	IA	0.1	10^{-4}	-	-	[65]

fact, device preparation and complexity, costs, possible toxicity and integrability in already existing manufacturing technologies have to be taken into account. AIE molecules have surprisingly high QY and g_{lum}, but the chiral aggregates responsible of these properties require effort in synthesising the molecular building block and can aggregate to the extent that the solubility decreases, compromising their processability. Also, their emission tunability is not straightforward. Liquid crystal systems show similar performance, even if in some cases the introduction of a new N*-LC layer is not desired, and thick-multilayered LC phases can be an obstacle for wearable and compact devices. Helicene and Pt-complex blends are perhaps the more elegant, cost effective and integrable technology, that can also exploit, in the case of transition metal complexes, the theoretical higher QY of phosphorescent organic light emitting diodes (PH-OLEDs).

When considering different type of applications, part of the aforementioned conditions does not have to be sought. In biomedical application, where high values of g_{lum} are considered positively to have high signal to noise ratio, more expensive systems based on Eu or thick liquid-crystals can be used. In this case, one of the main problems of lanthanide-based circularly polarized-LEDs (CP-LEDs) would be the narrow emission spectra, that might not overlap with the absorption of the studied tissue, drug or aggregate. However, the wide range of emission could be obtained combining these systems with wide band N*-LC multilayer reflectors, and their low efficiencies could be overcome with a bigger number of CP-LEDs in the active emitting matrix.

For secondary and more high-demanding applications, spin-LEDs and transition metal dichalcogenides (TDMs) based-devices represent unique devices. The former is an example of spin-information communication, the latter of electrically controlled polarization. Even if most of the times spin-LEDs require a magnetic field and vacuum technologies. And even if the preparation of low-dimensional TDMs is not yet scalable to an industrial level and the control was demonstrated only indirectly (the gating-gel needs to be frozen). These devices are widely studied, and their peculiar features could push for not yet invented technologies and applications.

With this work we explored and unveiled interesting features of circularly polarized light emission. A direct and absolute ranking comprising all different technologies is perhaps not appropriate, considering the different approaches, applications and secondary characteristics such as cost, manufacturing procedures and working principles. In addition, the comparison is in most of the cases not complete, taking into account that the data are only partially reported. Talking about this, the simultaneous communication of quantum efficiency, luminance and dissymmetry factors would increase the goodness of scientific advance. Furthermore, in some of the study the dissymetry factor is reported for materials in solution, in the solid state or integrated in LED device (electroluminescence, g_{EL}).

With this being said, having analysed most of the important approaches, doping achiral emitting materials with chiral molecules or complexes seems to be the more effective approach. However, the recent advances in the template-based approach, with the chiral template being affective also on a nanoscale[60] can result in thinner devices compared to the

cholesteric phase. This approach is also an example of tunable and wide spectral emission, that could also take benefits from many years of synthetic effort and optimization in the area of light emitting molecules and polymers.

We believe that, provided the intellectual honesty of reporting all the central data, this new generation of LEDs will introduce significant improvements in everyone's well-being and entrainment. Devices with helicene complexes, for which the requirements for a scalable and integrable technology have already been reached, are promising and research-pulling examples for tomorrow's applications.

Acknowledgements

I would personally like to thank Thomas la Cour Jansen for the time, the stimulating discussions and the wise suggestions provided during the supervision of this paper. In furnishing important tools, such as academic writing workshops and literature research, Ryan Chiechi and Maxim Pchenitchnikov were helpful and determined teachers (even if, the latter was not directly involved in the course). In conclusion, I would like to thank my bachelor classmate, Francesco Bignoli, and my flatmate, Saurabh Soni, for the stimulating feedbacks and discussions.

References

(1) Yang, Y.; Campbell, A. J.; da Costa, R. C.; Fuchter, M. J. *SID Symposium Digest of Technical Papers* **2013**, *44*, 4–7.

(2) Farshchi, R.; Ramsteiner, M.; Herfort, J.; Tahraoui, A.; Grahn, H. T. *Applied Physics Letters* **2011**, *98*.

(3) Tuchin, V. V. *Optical polarization in biomedical applications*; Springer: Berlin :, 2006.

(4) Zinna, F.; Pasini, M.; Galeotti, F.; Botta, C.; Di Bari, L.; Giovanella, U. *Advanced Functional Materials* **2016**, *1603719*.

(5) Schadt, M. *Annual Review of Materials Science* **1997**, *27*, 305–379.

(6) Muller, G. *Dalton transactions* **2009**, *322*, 9692–707.

(7) S-kei, Schematic diagrams of Light Emitting Diodes (LED). `https://commons.wikimedia.org/wiki/File%3APnJunction-LED-E.svg`, Accessed: 11.03.2017.

(8) Dave3457, Circularly polarized light with components (right handed). `https://commons.wikimedia.org/wiki/File:Circular.Polarization.Circularly.Polarized.Light{_}With.Components{_}Right.Handed.svg`, Accessed: 11.03.2017.

(9) Tang, C. W.; VanSlyke, S. A. *Applied Physics Letters* **1987**, *51*, 913–915.

(10) Berova, N.; Nakanishi, K.; Woody, R. *Circular dichroism: principles and applications*; Wiley-VCH, 2000; p 877.

(11) Eliel, E. L. E. L.; Wilen, S. H.; Mander, L. N. *Stereochemistry of organic compounds*; Wiley, 1994; p 1267.

(12) Condon, E. U. *Reviews of Modern Physics* **1937**, *9*, 432–457.

(13) Sánchez-Carnerero, E. M.; Agarrabeitia, A. R.; Moreno, F.; Maroto, B. L.; Muller, G.; Ortiz, M. J.; delaMoya, S. *Chemistry - A European Journal* **2015**, *21*, 13488–13500.

(14) Riehl, J. P.; Richardson, F. S. *Chemical Reviews* **1986**, *86*, 1–16.

(15) Didraga, C.; Pugžlys, A.; Hania, P. R.; Von Berlepsch, H.; Duppen, K.; Knoester, J. *Journal of Physical Chemistry B* **2004**, *108*, 14976–14985.

(16) Tempelaar, R.; Stradomska, A.; Knoester, J.; Spano, F. C. *The Journal of Physical Chemistry B* **2011**, *115*, 10592–10603.

(17) Spano, F. C.; Meskers, S. C. J.; Hennebicq, E.; Beljonne, D. *Journal of Chemical Physics* **2008**, *129*.

(18) Spano, F. C.; Zhao, Z.; Meskers, S. C. J. *The Journal of Chemical Physics* **2004**, *120*, 10594–10604.

(19) Kawamoto, H. *Proceedings of the IEEE* **2002**, *90*, 460–500.

(20) Chen, H.; Weng, Y.; Xu, D.; Tabiryan, N. V.; Wu, S.-T. *Optics Express* **2016**, *24*, 7287.

(21) Pu, L. *Acta polymerica* **2003**, *20*, 749–59.

(22) Langeveld-Voss, B. M. W.; Janssen, R. A. J.; Christiaans, M. P. T.; Meskers, S. C. J.; Dekkers, H. P. J. M.; Meijer, E. W. *Journal of the American Chemical Society* **1996**, *118*, 4908–4909.

(23) Langeveld-Voss, B. M. W.; Beljonne, D.; Shuai, Z.; Janssen, R. A. J.; Meskers, S. C. J.; Meijer, E. W.; Brédas, J.-L. *Advanced Materials* **1998**, *10*, 1343–1348.

(24) Peeters, E.; Christiaans, M. P. T.; Janssen, R. A. J.; Schoo, H. F. M.; Dekkers, H. P. J. M.; Meijer, E. W. *Journal of the American Chemical Society* **1997**, *119*, 9909–9910.
(25) Oda, M.; Nothofer, H.-G.; Lieser, G.; Scherf, U.; Meskers, S. C. J.; Neher, D. *Advanced Materials* **2000**, *12*, 362–365.
(26) Green, M. M.; Peterson, N. C.; Sato, T.; Teramoto, A.; Cook, R.; Lifson, S. *Science* **1995**, *268*, 1860–1866.
(27) Geng, Y.; Trajkovska, A.; Katsis, D.; Ou, J. J.; Culligan, S. W.; Chen, S. H. *Journal of the American Chemical Society* **2002**, *124*, 8337–47.
(28) Tang, H.-Z.; Fujiki, M.; Motonaga, M. *Polymer* **2002**, *43*, 6213–6220.
(29) Oda, M.; Nothofer, H. G.; Scherf, U.; Šunjić, V.; Richter, D.; Regenstein, W.; Neher, D. *Macromolecules* **2002**, *35*, 6792–6798.
(30) Geng, Y.; Trajkovska, A.; Culligan, S.; Ou, J.; Chen, P.; Katsis, D.; Chen, S. *Journal of the American Chemical Society* **2003**, 14032–14038.
(31) Wilson, J. N.; Steffen, W.; McKenzie, T. G.; Lieser, G.; Oda, M.; Neher, D.; Bunz, U. H. F. *Journal of the American Chemical Society* **2002**, *124*, 6830–6831.
(32) Dong, Y.; Lam, J. W. Y.; Qin, A.; Liu, J.; Li, Z.; Tang, B. Z.; Sun, J.; Kwok, H. S. *Applied Physics Letters* **2007**, *91*, 011111.
(33) Liu, J. Z.; Su, H. M.; Meng, L. M.; Zhao, Y. H.; Deng, C. M.; Ng, J. C. Y.; Lu, P.; Faisal, M.; Lam, J. W. Y.; Huang, X. H.; Wu, H. K.; Wong, K. S.; Tang, B. Z. *Chemical Science* **2012**, *3*, 2737–2747.
(34) Good, R. H.; Karali, A. *Journal of the Optical Society of America A* **1994**, *11*, 2145.
(35) Shi, H.; Conger, B. M.; Katsis, D.; Chen, S. H. *Liquid Crystals* **1998**, *24*, 163–172.
(36) Chen, S. H.; Katsis, D.; Schmid, A. W.; Mastrangelo, J. C.; Tsutsui, T.; Blanton, T. N. *Nature* **1999**, *397*, 506–508.
(37) de. Gennes, P. G.; Prost, J. *The physics of liquid crystals*; Clarendon Press, 1993.
(38) Bobrovsky, A.; Mochalov, K.; Oleinikov, V.; Sukhanova, A.; Prudnikau, A.; Artemyev, M.; Shibaev, V.; Nabiev, I. *Advanced Materials* **2012**, *24*, 6216–6222.
(39) Jeong, S. M.; Ohtsuka, Y.; Ha, N. Y.; Takanishi, Y.; Ishikawa, K.; Takezoe, H.; Nishimura, S.; Suzaki, G. *Applied Physics Letters* **2007**, *90*.
(40) Mitov, M. *Advanced Materials* **2012**, *24*, 6260–6276.
(41) Bobrovsky, A.; Boiko, N.; Shibaev, V.; Wendorff, J. *Advanced Materials* **2003**, *15*, 282–287.
(42) San Jose, B. A.; Matsushita, S.; Akagi, K. *Journal of the American Chemical Society* **2012**, *134*, 19795–19807.
(43) Iida, H.; Nakamura, A.; Inoue, Y.; Akagi, K. *Synthetic Metals* **2003**, *135-136*, 91–92.
(44) Chu, G.; Wang, X.; Chen, T.; Xu, W.; Wang, Y.; Song, H.; Xu, Y. *Journal of Material Chemistry C* **2015**, *3384*, 3384–3390.
(45) Haraguchi, S.; Numata, M.; Li, C.; Nakano, Y.; Fujiki, M.; Shinkai, S. *Chemistry Letters* **2009**, *38*, 254–255.
(46) Lakhwani, G.; Koeckelberghs, G.; Meskers, S. C. J.; Janssen, R. A. J. *Chemical Physics Letters* **2007**, *437*, 193–197.

(47) Furche, F.; Ahlrichs, R.; Wachsmann, C.; Weber, E.; Sobanski, A.; Vögtle, F.; Grimme, S. *Journal of the American Chemical Society* **2000**, *122*, 1717–1724.
(48) Yang, Y.; Da Costa, R. C.; Smilgies, D. M.; Campbell, A. J.; Fuchter, M. J. *Advanced Materials* **2013**, *25*, 2624–2628.
(49) Abbate, S. et al. *The Journal of Physical Chemistry C* **2014**, *118*, 1682–1695.
(50) Oyama, H.; Nakano, K.; Harada, T.; Kuroda, R.; Naito, M.; Nobusawa, K.; Nozaki, K. *Organic Letters* **2013**, *15*, 2104–2107.
(51) Baldo, M. A.; O'Brien, D. F.; Thompson, M. E.; Forrest, S. R. *Physical Review B* **1999**, *60*, 14422–14428.
(52) C. K. Luk and F. S. Richardson, *J. Am. Chem. Soc.* **1975**, *97*, 6666– 6675.
(53) Zinna, F.; Resta, C.; Abbate, S.; Castiglioni, E.; Longhi, G.; Mineo, P.; Di Bari, L. *Chemical Communication* **2015**, *51*, 11903–11906.
(54) Brandt, J. R.; Wang, X.; Yang, Y.; Campbell, A. J.; Fuchter, M. J. *Journal of the American Chemical Society* **2016**, *138*, 9743–9746.
(55) Lee, C. W.; Lee, J. Y. *Advanced Materials* **2013**, *25*, 5450–5454.
(56) Harada, T.; Tsumatori, H.; Nishiyama, K.; Yuasa, J.; Hasegawa, Y.; Kawai, T. *Inorganic Chemistry* **2012**, *51*, 6476–6485.
(57) Nakano, Y.; Liu, Y.; Fujiki, M. *Polym. Chem.* **2010**, *1*, 460–469.
(58) Jin, Y. J.; Kim, H.; Kim, J. J.; Heo, N. H.; Shin, J. W.; Teraguchi, M.; Kaneko, T.; Aoki, T.; Kwak, G. *Crystal Growth and Design* **2016**, *16*, 2804–2809.
(59) Feuillastre, S.; Pauton, M.; Gao, L.; Desmarchelier, A.; Riives, A. J.; Prim, D.; Tondelier, D.; Geffroy, B.; Muller, G.; Clavier, G.; Pieters, G. *Journal of the American Chemical Society* **2016**, *138*, 3990–3993.
(60) Goto, T.; Okazaki, Y.; Ueki, M.; Kuwahara, Y.; Takafuji, M.; Oda, R.; Ihara, H. *Angewandte Chemie International Edition* **2017**,
(61) Kioseoglou, G.; Petrou, A. *Journal of Low Temperature Physics* **2012**, *169*, 324–337.
(62) Holub, M.; Bhattacharya, P. *Journal of Physics D: Applied Physics* **2007**, *40*, 179–203.
(63) Hövel, S.; Gerhardt, N. C.; Hofmann, M. R.; Lo, F. Y.; Ludwig, A.; Reuter, D.; Wieck, A. D.; Schuster, E.; Wende, H.; Keune, W.; Petracic, O.; Westerholt, K. *Applied Physics Letters* **2008**, *93*, 2–5.
(64) Liang, S. H. et al. *Physical Review B* **2014**, *90*, 085310.
(65) Zhang, Y. J.; Oka, T.; Suzuki, R.; Ye, J. T.; Iwasa, Y. *Science* **2014**, *344*, 725–728.
(66) Cao, T.; Wang, G.; Han, W.; Ye, H.; Zhu, C.; Shi, J.; Niu, Q.; Tan, P.; Wang, E.; Liu, B.; Feng, J. *Nature Communications* **2012**, *3*, 887.
(67) Jones, A. M.; Yu, H.; Ghimire, N. J.; Wu, S.; Aivazian, G.; Ross, J. S.; Zhao, B.; Yan, J.; Mandrus, D. G.; Xiao, D.; Yao, W.; Xu, X. *Nature Nanotechnology* **2013**, *8*, 634–638.
(68) San Jose, B. a.; Akagi, K. *Polymer Chemistry* **2013**, *4*, 5144.
(69) Jiang, X.; Liu, X.; Jiang, Y.; Quan, Y.; Cheng, Y.; Zhu, C. *Macromolecular Chemistry and Physics* **2014**, *215*, 358–364.